Quantum sensing with an off the shelf super resolution microscope

Sangjun Noh [a], Minghao Jiang [b], Jocelyn Leon [f], Philip Hemmer [f], Peter J. Burke*[acde]
[a]Department of Electrical Engineering and Computer Science, University of California, Irvine, Irvine, CA 92697, USA; [b]Department of Physics and Astronomy, University of California, Irvine, Irvine, CA 92697, USA; [c]Department of Biomedical Engineering, University of California, Irvine, CA 92697; [d]Department of Chemical and Biomolecular Engineering, University of California, Irvine, CA 92697; [e]Department of Materials Science and Engineering, University of California, Irvine, CA 92697; [f]Department of Electrical and Computer Engineering, Texas A&M University, College Station, TX 77843-3128, USA

ABSTRACT

In this paper we present a simple method to demonstrate quantum sensing of magnetic fields with nitrogen vacancy centers in diamond using an off the shelf, commercial confocal and super resolution (Airyscan) microscope and a microwave generator. The measurement is based on CW (continuous wave) optically detected magnetic resonance (ODMR). The noise is empirically analyzed. This should give a good indication of what labs can expect with readily available microscopes in any modern university setting.

Keywords: NV center, OMDR, ZEISS Airyscan

1. INTRODUCTION

In this paper we present a simple method to demonstrate quantum sensing of magnetic fields with nitrogen vacancy centers in diamond[1] using an off the shelf, commercial confocal + super resolution[2,3] microscope and a microwave generator. The measurement is based on CW (continuous wave) optically detected magnetic resonance (ODMR). The noise is empirically analyzed. This should give a good indication of what labs can expect with readily available microscopes in any modern university setting.

2. MATERIAL AND METHOD

Microwave setup

Fig. 1a illustrates the microwave setup, which integrates a quantum sensing rack with a super-resolution microscope (ZEISS Airyscan LSM900). The quantum sensing rack generates and processes the microwave signal required for quantum experiments. A signal generator (Agilent N5181A) produces the initial signal, which is then amplified using a high-power amplifier (Mini-Circuits ZHL-16W-43-S+) and fine-tuned with a variable attenuator (Narda Microline 4704-99). To monitor the signal in real time, a 20 dB directional coupler (MAC Technology Inc.) and a spectrum analyzer (RIGOL DSA832E) are integrated into the setup at the output of the amplifier. All connections are established using SMA cables to ensure low-noise signal transmission and maintain system integrity.

Fig. 1b illustrates a diagram of microwave setup. A custom-fabricated omega-shaped microwave loop antenna was designed specifically for ODMR measurements of NV center diamonds[4]. The antenna exhibits a resonance frequency of 2.893 GHz with a bandwidth of 400 MHz, aligning precisely with the zero-field splitting frequency of the NV center. This configuration ensures efficient microwave delivery to the NV centers, optimizing the conditions for quantum state manipulation and measurement. To measure two peaks at 2.87 GHz, optimized +20 dBm output power was used for the ODMR measurement.

*pburke@uci.edu; phone 1 949 824-9326; fax 1 949 824-3732; burkelab.com

Quantum Effects and Measurement Techniques in Biology and Biophotonics II, edited by Clarice Aiello, Sergey V. Polyakov, Paige Derr, Proc. of SPIE Vol. 13340, 133400B
 · 1605-7422 · doi: 10.1117/12.3061587

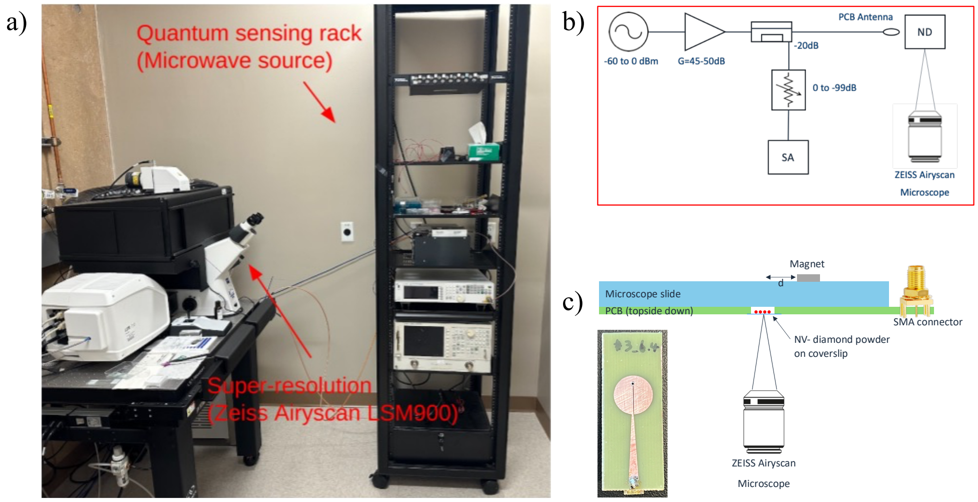

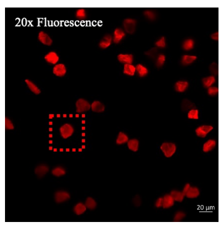

NV center diamond
Vendor: Adamas
Name: MDNV15umHi30mg
Size: 15µm diamond powder
NV ppm: ~3.5ppm

Figure 1. Integration of ODMR quantum sensing with super resolution microscope. a) Quantum sensing setup. b) Diagram of microwave setup. c) Schematic of the microwave antenna and NV center diamond. Subset is an omega loop antenna. d) Photoluminescent image of the NV center diamond

NV Center Diamond and External Magnetic Field

Fig. 1c shows a schematic of the omega-shaped antenna and the NV center diamond arrangement. NV center diamond powder (Adamas, MDNV15umHi30mg) was fixed to a coverslip (BIPEE, 12x12x0.13 mm) with a thin layer of CA super glue (Starbond, super fast thin) using the drop casting method. Then, the same super glue was used to fix it at the center of the omega loop antenna to ensure optimal interaction with the microwave field. To enable Zeeman splitting, a permanent magnet (N42, 10 × 4 × 2 mm) was placed directly above the antenna. Additional Zeeman splitting data with smaller magnetic fields generated by DC through a copper wire (AWG38) by adjusting current level were also measured. One novel method we developed is to deposit the nanodiamond directly on the copper wire creating the magnetic field. This has the advantage of keeping the quantum sensor as close as possible to the wire with minimal effort.

Airyscan and signal generator setup

We used the ZEISS in confocal mode, as the feature size did not require the Airyscan functionality. The ZEISS allows power to be set by the user as a percentage of full power (10 mW). We found an optimum power setting of 15% to excite NVs. To collect photoluminescence images while varying the microwave frequency from 2.7 to 3 GHz, synchronization between the Airyscan microscope and the signal generator is essential. After focusing on an NV center diamond, 201 images were acquired at a rate of 10 images/second. The images were 128x128 pixels with a dwell time of 1.52 µs per pixel. The signal generator sweep function was configured with identical interval and step point values to facilitate frequency sweeps. Once both systems were aligned, time-series images were acquired by initiating the Airyscan time-series function in tandem with the frequency sweep of the signal generator.

Imaging Analysis

The acquired time-series images were analyzed using FIJI (ImageJ) software. After importing the image series, the mean intensity of the entire field of view was calculated from the data and exported to a text file. The exported mean intensity data were subsequently plotted vs. microwave frequency using Igor Pro 9 software.

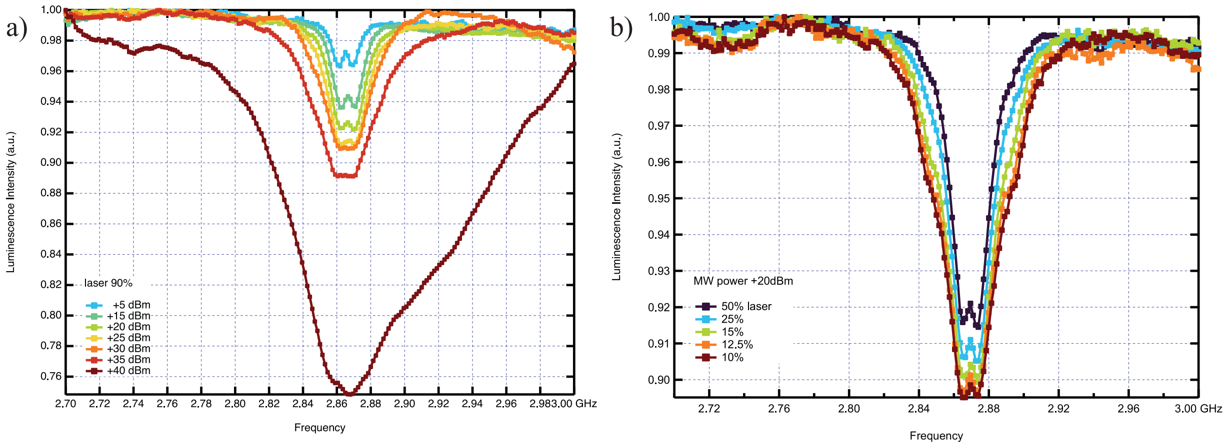

Figure 2. Laser and microwave power optimization. a) RF power optimization. +20 dBm shows the largest change with clear two peaks at 2.87 GHz. b) laser power optimization. The optimal laser power is 15% of 10 mW which had lowest standard deviation

3. RESULTS

ODMR vs optical, microwave power

Fig. 2 presents the ODMR results at various RF and optical powers. The optimal RF power is about +20 dBm, which shows the largest change while having two peaks. The optimal optical power is about 15% of the maximum power (100% is 10 mW), which shows the largest change at the resonant frequency and the smallest standard deviation at off-resonant frequency.

Zeeman splitting

Fig. 3 presents the ODMR results at different magnetic field strengths, demonstrating 2 peaks due to the Zeeman splitting. The ODMR measurements as a function of magnetic field were taken using either a permanent magnet or a magnetic field generated by DC current through a nearby copper wire, and all luminescence intensity data were normalized (arbitrary units, a.u.). The magnetic field from the permanent magnet was estimated from the geometry, and the magnetic field from the wire was calculates from the DC current using the Biot-Savart law.

Fig. 3a shows a typical Zeeman splitting pattern with up to eight peaks at an estimated magnetic field strength of 6.46 mT. In order to test a smaller magnetic field, the magnetic field was controlled through the DC current through wire in Fig. 3b. The field of view was adjusted to 20.46x20.46 µm which is slightly larger than the diamond size of 15 µm. By inspection by eye, the limit of detection (LOD) was 390 µT. In a second experiment, we zoomed in the field of view to be 8.25x8.25 µm, corresponding to the interior of the NV diamond, which lowered the updated LOD (by eye) to 79 µT in Fig. 3c.

Magnetic field sensitivity

A proper calculation of the magnetic field sensitivy would require a quantitative relationship between the measured noise on the flourescence intensity and the estimated magnetic field.[5] Here, we use a simple estimate for semi-quantitative purposes only. A full analysis will be published in the future.

The way that confocal microscopy works is a serial (in time) set of flourescent intensities is measured, one intensity at each pixel. The pixel dwell time is 1.52 µs, and our image size is 128x128 pixels. To interpret this as an effective measurement time and bandwidth, one can estimate the total integration time as 128x128x1.52 µs=25 ms. However, we need roughly 10 images to see the Zeeman split peak location, in order to estimate the magnetic field. Therefore, the measurement bandwidth would be 1/250 ms = 4 Hz, and the empirical magnetic field noise is 79 µT/√(4 Hz) ~ 40 µT /√Hz.

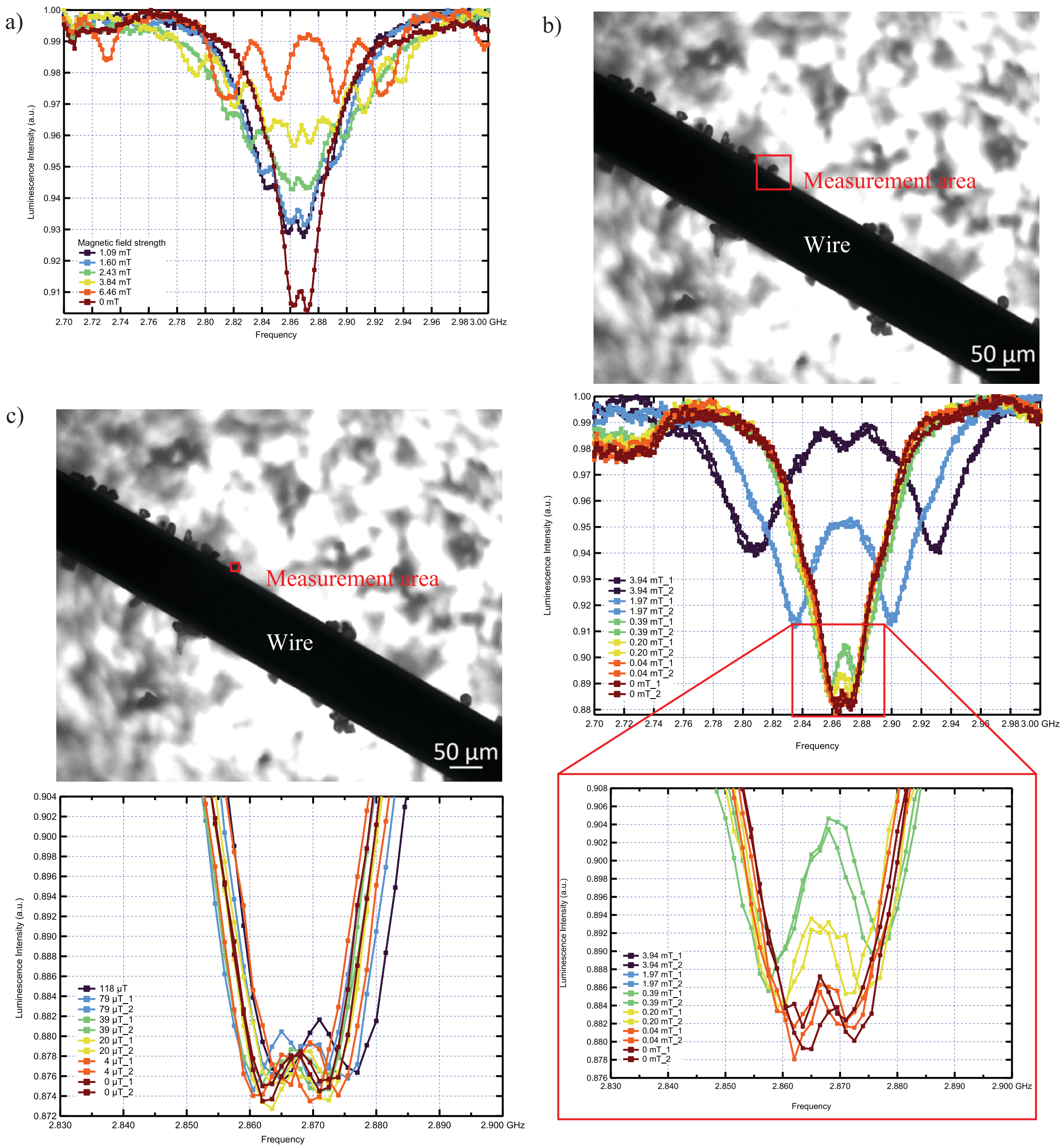

Figure 3. ODMR and Zeeman splitting. a) b) ODMR with a permanent magnet. Magnetic field strength was adjusted by changing the magnet position. c) ODMR with a variable magnetic field. A DC current through a copper wire was used to adjust magnetic field. d) ODMR with a wire in smaller ROI, 8.25x8.25 µm. Limit of detection was 79 µT.

4. DISCUSSION

Sensitivity comparison to state of the art

This paper demonstrates a magnetic field sensitivity of 40 µT /√Hz. A sensitivity of ~ pT/√Hz in $(0.5\ \text{mm})^3 = 10^{-10}\ \text{m}^3$ volume is typical state of the art best case[5,6]. In order to compare to state of the art magnetic field sensing as apples to apples, we need to normalize to the detection volume, i.e. the number of NV centers. We can either estimate the volume as one pixel, and use the total integration time (25 ms/image x 10 images), or we can estimate the volume as the total volume of pixels, and use the dwell term per pixel as the integration time. Above, we used the latter approach, so we will use that here also. Thus, our detection volume in Fig. 3c corresponds to 1 pixel, which we estimate as a diffraction limited cube of side 1 μm, for an effective volume of 10^{-18} m^3. Scaling this to 10^{-10} m^3 would give rise to $\sqrt{(10^8)}$ less noise (since the noise scales as the square root of the number of NV centers, resulting in 4 nT /√Hz. This demonstrates what can readily be achieved in any modern lab with a confocal microscope and small amount of effort.

5. CONCLUSION

Several recent papers have provided detailed recipes for setting up quantum sensing and quantum state manipulation with NV sensors in diamond. Sewani et al[7] provided complete, detailed instructions on how to create a tabletop quantum state manipulation setup, including coherent pulse manipulation and Rabi oscillations, on ensembles of NV centers for around $10k. A lower cost setup for under $500 to observe CW ODMR was presented by Zhang et al[8]. At the high end, Misonou et al[9], and more recently Yuan et al[10] provided detailed instructions for single NV center, single photon sensitive, quantum state manipulation with a home made confocal microscope for $100k or more. In contrast to those works, this paper presents a method to use an off-the shelf commercial confocal microscope, or an off the shelf super-resolution microscope, to develop experiments in quantum sensing with only a small amount of easily obtainable RF equipment. While we used a commercial RF generator, this could easily be replaced with a USB Windfreak (SynthUSB3) for around $400, and so the main cost would be the 1 Watt power amplifier, at around $2000. The antenna can be made cheaply in house or via one of a number of commercial PCB manufacturers for under $100. A disadvantage of this approach is the closed source nature of the ZEISS ecosystem. The user cannot get access to the photodector current, or the laser timing. This prevents time domain quantum state manipulation with this system. With the growth of emerging application of optical, room temperature quantum state manipulation in quantum sensing and quantum information, it would seem there would be a significant commercial opportunity for optical quantum state manipulation systems. We have found, in discussions with many different microscope manufacturers and optics companies, including household name companies as well as nimble startups with the world's best super resolution systems, that they do not allow such access. Therefore, for time domain quantum state manipulation of optical spin-based quantum bits, to our knowledge, the only solution available as of this writing (February 2025) is to do it yourself, a project currently in progress in our lab. For applications where time domain quantum state manipulation is not needed, this paper presents a much easier route towards CW quantum sensing with off the shelf, readily available microscopes.

ACKNOWLEDGEMENTS

This work was supported by the Air Force Office of Scientific Research (AFOSR) under awards FA9550-23-1-0061 and FA9550-23-1-0436, and also in part by the National Science Foundation (NSF) under Award 2153425, and the Noyce Foundation. Any opinions, findings, and conclusions or recommendations expressed in this material are those of the author(s) and do not necessarily reflect the views of the United States Air Force.

REFERENCES

[1] Romana Schirhagl, Kevin Chang, Michael Loretz, and Christian L. Degen, "Nitrogen-vacancy centers in diamond: Nanoscale sensors for physics and biology," Annu Rev Phys Chem 65, 83–105, Annual Reviews Inc. (2014); http://dx.doi.org/10.1146/annurev-physchem-040513-103659

[2] Lothar Schermelleh, Alexia Ferrand, Thomas Huser, Christian Eggeling, Markus Sauer, Oliver Biehlmaier, and Gregor P. C Drummen, "Super-resolution microscopy demystified" (2 January 2019); http://dx.doi.org/10.1038/s41556-018-0251-8

[3] Joseph Huff, "The Airyscan detector from ZEISS: confocal imaging with improved signal-to-noise ratio and super-resolution" (1 December 2015); http://dx.doi.org/10.1038/nmeth.f.388

[4] Kento Sasaki, Yasuaki Monnai, Soya Saijo, Ryushiro Fujita, Hideyuki Watanabe, Junko Ishi-Hayase, Kohei M. Itoh, and Eisuke Abe, "Broadband, large-area microwave antenna for optically detected magnetic resonance of nitrogen-vacancy centers in diamond," Review of Scientific Instruments 87(5), American Institute of Physics Inc. (26 May 2016); http://dx.doi.org/10.1063/1.4952418

[5] John F. Barry, Jennifer M. Schloss, Erik Bauch, Matthew J. Turner, Connor A. Hart, Linh M. Pham, and Ronald L. Walsworth, "Sensitivity optimization for NV-diamond magnetometry," Rev Mod Phys 92(1), 015004, American Physical Society (31 March 2020); http://dx.doi.org/10.1103/RevModPhys.92.015004

[6] Chen Zhang, Farida Shagieva, Matthias Widmann, Michael Kübler, Vadim Vorobyov, Polina Kapitanova, Elizaveta Nenasheva, Ruth Corkill, Oliver Rhrle, Kazuo Nakamura, Hitoshi Sumiya, Shinobu Onoda, Junichi Isoya, and Jörg Wrachtrup, "Diamond Magnetometry and Gradiometry towards Subpicotesla dc Field Measurement," Phys Rev Appl 15(6), 064075, American Physical Society (30 June 2021); http://dx.doi.org/10.1103/PhysRevApplied.15.064075

[7] Vikas K. Sewani, Hyma H. Vallabhapurapu, Yang Yang, Hannes R. Firgau, Chris Adambukulam, Brett C. Johnson, ; Jarryd, J. Pla, Arne Laucht, John Essick, and Jarryd J. Pla, "Coherent control of NV− centers in diamond in a quantum teaching lab," Am J Phys 88(12), 1156–1169, AIP Publishing (1 December 2020); http://dx.doi.org/10.1119/10.0001905

[8] Haimei Zhang, Carina Belvin, Wanyi Li, Jennifer Wang, Julia Wainwright, Robbie Berg, Joshua Bridger, and John Essick, "Little bits of diamond: Optically detected magnetic resonance of nitrogen-vacancy centers," Am J Phys 86(3), 225–236, AIP Publishing (1 March 2018); http://dx.doi.org/10.1119/1.5023389

[9] Daiki Misonou, Kento Sasaki, Shuntaro Ishizu, Yasuaki Monnai, Kohei M. Itoh, and Eisuke Abe, "Construction and operation of a tabletop system for nanoscale magnetometry with single nitrogen-vacancy centers in diamond," AIP Adv 10(2), 25206, American Institute of Physics Inc. (5 February 2020); http://dx.doi.org/10.1063/1.5128716

[10] Zhiyang Yuan, Sounak Mukherjee, Aedan Gardill, Jeff D. Thompson, Shimon Kolkowitz, and Nathalie P. de Leon, "An instructional lab apparatus for quantum experiments with single nitrogen-vacancy centers in diamond," Am J Phys 92(11), 892–900, AIP Publishing (1 November 2024); http://dx.doi.org/10.1119/5.0216511